
WASSERSTEIN GRADIENT FLOW OVER VARIATIONAL PARAMETER SPACE FOR VARIATIONAL INFERENCE

A PREPRINT

Dai Hai Nguyen

Department of Computer Science
University of Tsukuba, Japan
hai@cs.tsukuba.ac.jp

Tetsuya Sakurai

Department of Computer Science
University of Tsukuba, Japan
sakurai@cs.tsukuba.ac.jp

Hiroshi Mamitsuka

Bioinformatics Center
Kyoto University, Japan
mami@kuicr.kyoto-u.ac.jp

October 26, 2023

ABSTRACT

Variational inference (VI) can be cast as an optimization problem in which the variational parameters are tuned to closely align a variational distribution with the true posterior. The optimization task can be approached through vanilla gradient descent in black-box VI or natural-gradient descent in natural-gradient VI. In this work, we reframe VI as the optimization of an objective that concerns probability distributions defined over a *variational parameter space*. Subsequently, we propose Wasserstein gradient descent for tackling this optimization problem. Notably, the optimization techniques, namely black-box VI and natural-gradient VI, can be reinterpreted as specific instances of the proposed Wasserstein gradient descent. To enhance the efficiency of optimization, we develop practical methods for numerically solving the discrete gradient flows. We validate the effectiveness of the proposed methods through empirical experiments on a synthetic dataset, supplemented by theoretical analyses.

1 Introduction

Many machine learning problems involve the challenge of approximating an intractable target distribution, which might only be known up to a normalization constant. Bayesian inference is a typical example, where the intractable and unnormalized target distribution is a result of the product of the prior and likelihood functions (see [11, 18, 4]). Variational Inference (VI), a widely employed across various application domains, seeks to approximate this intractable target distribution by utilizing a variational distribution (see [3, 7, 20] and references therein). VI is typically formulated as an optimization problem, with the objective of maximizing the evidence lower bound objective (ELBO), which is equivalent to minimizing the Kullback-Leiber (KL) divergence between the variational distribution and the target distribution.

The conventional method for maximizing the ELBO involves the use of gradient descent, such as black-box VI (BBVI, [16]). The gradient of the ELBO can be expressed as an expectation over the variational distribution, which is typically estimated by Monte Carlo samples from this distribution. However, it is worth noting that the gradient estimator can sometimes be excessively large, making it less practical for optimization purposes. In contrast, natural-gradient-based methods, such as natural-gradient VI (NGVI, [9]) has demonstrated its superior efficiency compared to the standard gradient descent for VI. The natural-gradient, introduced in [1], can be obtained from the vanilla gradient by preconditioning it with the inverse of the Fisher information matrix (FIM). However, explicitly computing this inverse FIM can be computationally expensive in general cases. An interesting fact highlighted in [9] is that the natural gradient concerning the natural parameters of an exponential family distribution (e.g., Gaussian) is equivalent to the standard gradient concerning the expectation parameters. This equivalence simplifies the updates and often leads to faster convergence compared to gradient-based methods. Nevertheless, the natural-gradient methods generally do not accept simple updates when dealing with mixture models such as a Gaussian mixture. This presents a challenge in extending the efficiency gains of natural-gradient techniques to such complex models.

Our work is based on the notions of gradient flows in the space of probability distributions, called Wasserstein gradient flows (WGF), which is first introduced in [8]. Essentially, WGF induces a geometry structure (manifold) in the distribution space characterized by a functional. The distance between two elements on the manifold is defined by the second-order Wasserstein (or 2-Wasserstein) distance. A gradient flow within this context corresponds to a sequence of distributions which progressively converge towards an optimal distribution during an iterative optimization process. Prior to our work, several recent studies also apply WGFs to VI. For instance, in [10], the focus is on Gaussian VI, where the goal is to approximate the target distribution by finding the closest Gaussian distribution within the Gaussian distribution family. Since the Gaussian distribution family is parametric, the gradient flow is defined within the Bures-Wasserstein space of Gaussian distributions, constructing a sequence of Gaussian distributions that converges to the target distribution. Similarly, in [19], the focus is on mean-field VI, where the entire space of factorized probability distributions is considered. Here, a sequence of factorized distributions is constructed in a manner that they progressively converge to the optimal distribution.

We adopt a novel approach, which is distinct from the methods mentioned above. Those existing methods define probability distributions over the *latent variable space*, possibly with limitations, for example, when capturing multi-modal target distributions. While our approach defines probability distributions over the *variational parameter space*, without such limitations. More substantially, we can reframe the optimization of VI with respect to the variational parameters into a distributional optimization task, involving probability distributions over the variational parameters. Subsequently, we apply variants of WGF to the computation of VI. In summary, we can raise the following three merits of our method, which allows

- 1) to provide a *unified perspective on BBVI and NGVI*, demonstrating that both updates precisely emerge as the particle approximations of a gradient flow defined over variational parameter space (as shown in (16)), particularly when the number of particles is set to one.
- 2) BBVI and NGVI to *handle mixture models*, such as a mixture of Gaussian distributions, by using multiple particles, where each particle represents a component. This enhances their ability to approximate complex and multi-modal target distributions.
- 3) to *establish theoretical insights* into the developed methods, leveraging well-established theories of gradient flows. This deepens our understanding of how our methods behave and operate.

The rest of this paper is organised as follows: in Section 2, we review BBVI and NGVI, the two common gradient-based optimization methods for VI, and then introduce necessary background of gradient flows on a probability measure space; in Section 3, we present our novel approach for interpreting VI as a distributional optimization defined on the parameter space and develop methods for the optimization based on variants of WGFs; in Section 4, we report experimental results on a synthetic data set, demonstrating the effectiveness of the proposed method; finally, we conclude our work in Section 5.

2 Related Work

We first review BBVI and NGVI, the two common gradient-based optimization methods for VI. Then, we review backgrounds on gradient flows on the probability measure space, which we use to reinterpret the two mentioned methods.

2.1 Gradient-based Optimization for VI

We consider the following problem setting. Let D be a set of observations, \mathbf{z} be a latent variable and $q(\mathbf{z}|\boldsymbol{\lambda})$ be the variational distribution with the variational parameter $\boldsymbol{\lambda} \in \mathbb{R}^d$, our goal is to approximate the true posterior $p(\mathbf{z}|D)$ with q by solving the following problem of minimizing the negated ELBO:

$$\min_{\boldsymbol{\lambda}} \mathcal{L}(\boldsymbol{\lambda}) = E_{\mathbf{z} \sim q(\cdot|\boldsymbol{\lambda})} [f(\mathbf{z}) - H(q)], \quad (1)$$

where $f(\mathbf{z}) = -\log p(D, \mathbf{z})$ and $H(q)$ is the entropy of q , given by: $H(q) = -\mathbb{E}_{\mathbf{z} \sim q(\cdot|\boldsymbol{\lambda})} [\log q(\mathbf{z}|\boldsymbol{\lambda})]$.

The negated ELBO (see (1)) can be straightforwardly optimized with the gradient descent algorithm, known as BBVI [16]. To do this, we need to estimate the gradient of negated ELBO as an expectation to the variational distribution $q(\mathbf{z}|\boldsymbol{\lambda})$:

$$\begin{aligned} \boldsymbol{\lambda}_{t+1} &\leftarrow \boldsymbol{\lambda}_t - \eta \nabla_{\boldsymbol{\lambda}} \mathcal{L}(\boldsymbol{\lambda}_t), \\ \nabla_{\boldsymbol{\lambda}} \mathcal{L}(\boldsymbol{\lambda}) &= \mathbb{E}_{\mathbf{z} \sim q(\cdot|\boldsymbol{\lambda})} [\nabla_{\boldsymbol{\lambda}} \log q(\mathbf{z}|\boldsymbol{\lambda}) (f(\mathbf{z}) + \log q(\mathbf{z}|\boldsymbol{\lambda}))], \end{aligned} \quad (2)$$

where η is the learning rate, and the gradient of the negated ELBO, $\nabla_{\lambda} \mathcal{L}$, can be estimated using Monte Carlo samples from $q(\mathbf{z}|\lambda)$. However, compared to the gradient descent, natural-gradient descent [1] has been shown to be much more efficient for VI [9]. The natural gradient can be obtained from the standard gradient by preconditioning it with the inverse Fisher Information Matrix (FIM). However, explicitly computing the FIM can be computationally expensive. As a more efficient alternative, [9] has shown that the natural-gradient with respect to the natural parameters of an exponential family distribution (such as Gaussian) is equivalent to the standard gradient with respect to the expectation parameters:

$$\begin{aligned}\lambda_{t+1} &\leftarrow \lambda_t - \eta [\mathbf{F}(\lambda_t)]^{-1} \nabla_{\lambda} \mathcal{L}(\lambda_t) \\ \lambda_{t+1} &\leftarrow \lambda_t - \eta \nabla_{\mathbf{m}} \mathcal{L}(\lambda_t),\end{aligned}\tag{3}$$

where $\mathbf{F}(\lambda)$ is the FIM with respect to the natural parameter λ , and \mathbf{m} is the expectation parameter of the exponential-family distribution, given by: $\mathbf{m}(\lambda) = \mathbb{E}_{\mathbf{z} \sim q(\cdot|\lambda)} [T(\mathbf{z})]$, where $T(\mathbf{z})$ is the sufficient statistics of q (see [3] for reference). For VI, the gradient of negated ELBO with respect to the expectation parameter is shown to be much more efficient. For instance, when q is a mean-field Gaussian distribution, i.e., $q(\mathbf{z}|\lambda) = \mathcal{N}(\mathbf{z}|\mu, \sigma^2)$, the update of NGVI is obtained as follows:

$$\begin{aligned}\mu_{t+1} &\leftarrow \mu_t - \eta \sigma_{t+1}^2 \odot \nabla_{\mathbf{z}} f(\mathbf{z}), \\ \sigma_{t+1}^{-2} &\leftarrow (1 - \eta) \sigma_t^{-2} + \eta \text{diag} [\nabla_{\mathbf{z}\mathbf{z}}^2 f(\mathbf{z})],\end{aligned}\tag{4}$$

where $\mathbf{a} \odot \mathbf{b}$ denotes the element-wise product between vectors \mathbf{a} and \mathbf{b} and $\text{diag}[\mathbf{A}]$ denotes the function to extract diagonal entries of matrix \mathbf{A} .

2.2 Gradient Flows on Probability Measure Space

Consider to minimize $F : \mathcal{P}(\Omega) \rightarrow \mathbb{R}$, a functional in the space of probability measures $\mathcal{P}(\Omega)$ with $\Omega \subset \mathbb{R}^d$. We first endow a Riemannian geometry on $\mathcal{P}(\Omega)$. The geometry is characterized by the distance between two distributions, defined by the 2-Wasserstein distance:

$$\mathcal{W}_2^2(p, p') = \inf_{\pi \in \Pi(p, p')} \int_{\Omega \times \Omega} \|\mathbf{x} - \mathbf{x}'\|_2^2 d\pi(\mathbf{x}, \mathbf{x}'),$$

where $\Pi(p, p')$ is the set of joint distributions over $(\mathbf{x}, \mathbf{x}')$ such that the two marginals equal p and p' , respectively. This is an optimal transport problem, which has received much attention in the machine learning community and has been shown to be an effective tool for comparing probability distributions in many applications (see [15, 14, 13] for examples). If p is absolutely continuous with respect to the Lebesgue measure, there exists a unique optimal transport plan from p to p' , i.e., a mapping $T : \Omega \rightarrow \Omega$ pushing p onto p' satisfying $p' = T\#p$, where $T\#p$ denotes the pushforward measure of p . Then, the Wasserstein distance is equivalently reformulated as:

$$\mathcal{W}_2^2(p, p') = \inf_T \int_{\Omega} \|\mathbf{x} - T(\mathbf{x})\|_2^2 dp(\mathbf{x}).$$

Let $\{p_t\}_{t \in [0, 1]}$ be an absolutely continuous curve in $\mathcal{P}(\Omega)$ with finite second-order moments and define $\mathbf{v}_t(\mathbf{x}) = \lim_{h \rightarrow 0} \frac{T(\mathbf{x}_t) - \mathbf{x}_t}{h}$ as the velocity of the particle, a gradient flow on $\mathcal{P}(\Omega)$ can be defined as $\partial_t p_t + \text{div}(p_t \mathbf{v}_t) = 0$, where div is the divergence operator. It can be shown that F is the functional of a gradient flow on $\mathcal{P}(\Omega)$, then \mathbf{v}_t has the following form: $\mathbf{v}_t = -\nabla \frac{\delta F}{\delta p_t}(p_t)$ [17], where $\frac{\delta F}{\delta p_t}$ is the first variation of F at p_t . Based on this, gradient flows on $\mathcal{P}(\Omega)$ can be expressed as follows:

$$\partial_t p_t = -\text{div}(p_t \mathbf{v}_t) = \text{div} \left(p_t \nabla \left(\frac{\delta F}{\delta p_t}(p_t) \right) \right).\tag{5}$$

Remark 1 The gradient flow (5) defines a solution path on $\mathcal{P}(\Omega)$ to minimize F . If F is geodesically convex, the globally optimal convergence is guaranteed.

3 Gradient Flows over Variational Parameter Space for VI

3.1 A Novel Perspective from Gradient Flows over Variational Parameter Space

Our perspective is motivated from the key question: how to extend BBVI and NGVI to the case where the variational distribution is assumed to be a mixture of distributions (such as a mixture of Gaussian distributions) in a principled way.

To this end, we adopt a novel approach that differs from the previous methods. Our approach is designed to address the challenges mentioned above by introducing a probability distribution p over the variational parameters $\{\lambda_k\}_{k=1}^K$ as follows:

$$p(\boldsymbol{\lambda}) = \frac{1}{K} \sum_{k=1}^K \delta_{\lambda_k}(\boldsymbol{\lambda}). \quad (6)$$

Then, the variational distribution $q(\mathbf{z})$ is expressed as follows:

$$q(\mathbf{z}) = \mathbb{E}_{\boldsymbol{\lambda} \sim p} [q(\mathbf{z}|\boldsymbol{\lambda})] = \frac{1}{K} \sum_{k=1}^K q(\mathbf{z}|\lambda_k). \quad (7)$$

As a result, we can reformulate the negated ELBO with respect to variational parameters into a distributional optimization problem with respect to p over variational parameters as follows:

$$\min_{p \in \mathcal{P}(\Omega)} \mathcal{L}(p) = \mathbb{E}_{\boldsymbol{\lambda} \sim p} \mathbb{E}_{\mathbf{z} \sim q(\cdot|\boldsymbol{\lambda})} [f(\mathbf{z}) + \log q(\mathbf{z})], \quad (8)$$

where Ω denotes the variational parameter space and $\mathcal{P}(\Omega)$ denotes the set of distributions over variational parameters in the context of our work.

Remark 2. It is noteworthy that both VI, as expressed in (2) and our reformulated problem, as expressed in (8), involve the optimization over probability measure spaces. However, the fundamental distinction lies in the definitions of the domain Ω : in (2), the optimization variable is the variational distribution $q(\mathbf{z}|\boldsymbol{\lambda})$, which is defined within the domain of samples \mathbf{z} , while in (8), the variable is p , which is defined within the spaces of variational parameters $\boldsymbol{\lambda}$. This distinction makes our approach novel.

The following theorem shows the first variation of $\mathcal{L}(p)$. This is particularly useful in formulating the gradient flows on the probability measure space of variational parameters.

Theorem 1. (First variation of $\mathcal{L}(p)$). *The first variation of $\mathcal{L}(p)$ defined in (8) is given by:*

$$\frac{\delta \mathcal{L}}{\delta p}(\boldsymbol{\lambda}) = \mathbb{E}_{\mathbf{z} \sim q(\cdot|\boldsymbol{\lambda})} [f(\mathbf{z}) + \log (\mathbb{E}_{\boldsymbol{\lambda} \sim p} [q(\mathbf{z}|\boldsymbol{\lambda})])] + 1, \quad (9)$$

which can be approximated using Monte Carlo samples:

$$\frac{\delta \mathcal{L}}{\delta p}(\boldsymbol{\lambda}) \approx \frac{1}{N} \sum_{i=1}^N f(\mathbf{z}_i) + \log \left(\frac{1}{K} \sum_{k=1}^K q(\mathbf{z}_i|\lambda_k) \right) + 1,$$

where $\boldsymbol{\lambda}_k \sim p$, $k = 1, 2, \dots, K$ and $\mathbf{z}_i \sim q(\cdot|\boldsymbol{\lambda})$, $i = 1, \dots, N$.

The proof of Theorem 1 can be found in the supplementary material. Our objective is to establish gradient flows over probability distribution spaces, where the domain Ω is defined over variational parameters. The Wasserstein gradient flow is essentially a curve $(p_t)_{t \geq 0}$ that satisfies (5). In this work, we introduce a generalized variational parameter flow as follows:

$$\frac{\partial \boldsymbol{\lambda}_t}{\partial t} = -\mathbf{C}(\boldsymbol{\lambda}_t) \nabla \frac{\delta \mathcal{L}}{\delta p_t}(\boldsymbol{\lambda}_t), \quad (10)$$

where $\mathbf{C}(\boldsymbol{\lambda}) \in \mathbb{R}^{d \times d}$ is a positive-definite matrix. We consider two typical cases: 1) $\mathbf{C}(\boldsymbol{\lambda}) = \mathbf{I}_d$, where \mathbf{I}_d is the identity matrix, and 2) $\mathbf{C}(\boldsymbol{\lambda}) = \mathbf{F}^{-1}(\boldsymbol{\lambda})$, where $q(\mathbf{z}|\boldsymbol{\lambda})$ is assumed to be an exponential-family distribution and $\boldsymbol{\lambda}$ is its natural parameter. Then, the dynamic of p_t , the probability distribution of $\boldsymbol{\lambda}_t$, is induced by the following continuity equation:

$$\frac{\partial p_t}{\partial t} + \text{div}(p_t \mathbf{C} \mathbf{v}_t) = 0, \mathbf{v}_t = -\nabla \frac{\delta \mathcal{L}}{\delta p_t}. \quad (11)$$

Continuous-time dynamics. We propose to study the dissipation of $\mathcal{L}(p_t)$ along the trajectory of the flow (11), as stated in the following proposition.

Proposition 2. (Continuous-time dynamics). *The dissipation of \mathcal{L} along the gradient flow (11) is characterized as follows:*

$$\frac{d\mathcal{L}(p_t)}{dp_t} = -\langle \mathbf{v}_t, \mathbf{C} \mathbf{v}_t \rangle_{L^2(p_t)}, \quad (12)$$

where $L^2(p)$ denotes the space of function $h : \Omega \rightarrow \Omega$, and $\langle \cdot, \cdot \rangle_{L^2(p)}$ denotes the inner product of $L^2(p)$.

Proof. Using differential calculus in the Wasserstein space and the chain rule, we have:

$$\begin{aligned} \frac{d\mathcal{L}(p_t)}{dp_t} &= - \int_{\boldsymbol{\lambda}} \frac{\delta \mathcal{L}}{\delta p_t}(\boldsymbol{\lambda}) \operatorname{div}(p_t \mathbf{C} \mathbf{v}_t) d\boldsymbol{\lambda} \\ &= \int_{\boldsymbol{\lambda}} \langle \mathbf{C}(\boldsymbol{\lambda}) \mathbf{v}_t(\boldsymbol{\lambda}), \nabla \frac{\delta \mathcal{L}}{\delta p_t}(\boldsymbol{\lambda}) \rangle dp_t(\boldsymbol{\lambda}) \\ &= - \int_{\boldsymbol{\lambda}} \langle \mathbf{v}_t(\boldsymbol{\lambda}), \mathbf{C}(\boldsymbol{\lambda}) \mathbf{v}_t(\boldsymbol{\lambda}) \rangle dp_t(\boldsymbol{\lambda}). \end{aligned}$$

□

Since \mathbf{C} is positive-definite matrix, the right-hand side of (12) is non-negative. Thus Proposition 2 indicates that \mathcal{L} with respect to p_t decreases along the gradient flow (11). The second consequence is the following corollary.

Corollary. *For any $t > 0$, we have:*

$$\min_{0 \leq s \leq t} \langle \mathbf{v}_s, \mathbf{C} \mathbf{v}_s \rangle_{L^2(p_s)} \leq \frac{1}{t} \int_0^t \langle \mathbf{v}_s, \mathbf{C} \mathbf{v}_s \rangle_{L^2(p_s)} ds \leq \frac{\mathcal{L}(p_0)}{t}.$$

The corollary indicates that the gradient norm will converge to zero as t goes to infinite. However, it is not guaranteed that it converges to the globally optimal solution because of the non-convexity of \mathcal{L} .

Discrete-time dynamics. Next we study the dissipation of \mathcal{L} in discrete time. We consider the following gradient descent update in the Wasserstein space applied to \mathcal{L} at each iteration $n \geq 0$:

$$p_{n+1} = (\mathbf{I} - \eta \mathbf{C} \mathbf{v}_n) \# p_n, \quad (13)$$

where \mathbf{I} is the identity map. This update corresponds to a forward Euler discretization of the gradient flow (11). Let $p_0 \in \mathcal{P}_2(\Omega)$ be the initial distribution of parameter $\boldsymbol{\lambda}_0$, i.e. $\boldsymbol{\lambda}_0 \sim p_0$. For every $n > 0$, $\boldsymbol{\lambda}_n \sim p_n$, we have:

$$\boldsymbol{\lambda}_{n+1} = \boldsymbol{\lambda}_n - \eta \mathbf{C}(\boldsymbol{\lambda}_n) \mathbf{v}_n(\boldsymbol{\lambda}_n). \quad (14)$$

We study the dissipation of $\mathcal{L}(p_n)$ along the gradient update (14) in the infinite number of particles regimes (where K goes to infinity). We intend to obtain a descent lemma similar to Proposition 2. However, the discrete-time analysis requires more assumptions than the continuous-time analysis. Here we assume the following for all $\boldsymbol{\lambda}$:

(A1) Assume $\exists \alpha_1, \alpha_2 > 0$ s.t.

$$\begin{aligned} \mathbb{E}_{\mathbf{z} \sim q(\cdot | \boldsymbol{\lambda})} \|\nabla_{\boldsymbol{\lambda}} \log q(\mathbf{z} | \boldsymbol{\lambda})\|_2^2 &\leq \alpha_1, \\ \mathbb{E}_{\mathbf{z} \sim q(\cdot | \boldsymbol{\lambda})} \|\nabla_{\boldsymbol{\lambda}} \log q(\mathbf{z})\|_2^2 &\leq \alpha_2. \end{aligned}$$

(A2) Assume $\exists \beta_1, \beta_2 > 0$ s.t.

$$\begin{aligned} \mathbb{E}_{\mathbf{z} \sim q(\cdot | \boldsymbol{\lambda})} \|\nabla_{\boldsymbol{\lambda}}^2 \log q(\mathbf{z} | \boldsymbol{\lambda})\|_{\text{op}} &\leq \beta_1, \\ \mathbb{E}_{\mathbf{z} \sim q(\cdot | \boldsymbol{\lambda})} \|\nabla_{\boldsymbol{\lambda}}^2 \log q(\mathbf{z})\|_{\text{op}} &\leq \beta_2, \end{aligned}$$

where $\|\mathbf{A}\|_{\text{op}} = \sup_{\|\mathbf{u}\|_2=1} \|\mathbf{A}\mathbf{u}\|_2$ is the operator norm of matrix \mathbf{A} .

(A3) Assume $\exists M_1, M_2 > 0$ s.t.

$$\mathbb{E}_{\mathbf{z} \sim q(\cdot | \boldsymbol{\lambda})} |f(\mathbf{z})| \leq M_1, \mathbb{E}_{\mathbf{z} \sim q(\cdot | \boldsymbol{\lambda})} |\log q(\mathbf{z})| \leq M_2$$

Given our assumptions, we quantify the decreasing of \mathcal{L} along the gradient update (14), as stated in the following descent lemma.

Proposition 3. *(Descent lemma for discrete-time dynamics). Assume (A1), (A2) and (A3) hold. Let $\kappa = (\alpha_1 + \beta_1)(M_1 + M_2) + \alpha_1 + \alpha_2 + \beta_2$, and choose sufficiently small learning rate $\eta < 2/\kappa$. Then we have:*

$$\mathcal{L}(p_{n+1}) - \mathcal{L}(p_n) \leq -\eta \left(1 - \kappa \frac{\eta}{2}\right) \langle \mathbf{v}_n, \mathbf{C} \mathbf{v}_n \rangle_{L^2(p_n)}. \quad (15)$$

Proof of Proposition 3 can be found in the supplementary material. Proposition 3 indicates that the objective $\mathcal{L}(p_n)$ decreases by the gradient update (14) since the right-hand side of (15) is non-positive by choosing a sufficiently small learning rate and the positive-definiteness of \mathbf{C} . The following corollary is the direct consequence from the descent lemma.

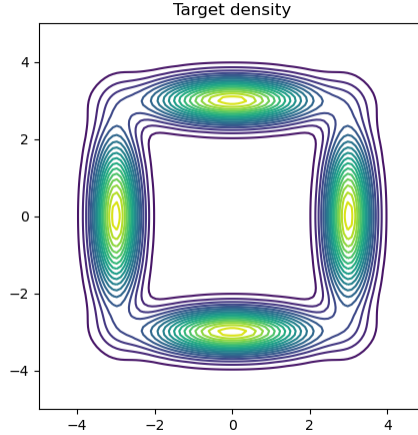


Figure 1: The contour plot of the target distribution (mixture of four Gaussian distributions)

Corollary. Let $\eta < 2/\kappa$ and $c_\eta = \eta(1 - \kappa \frac{\eta}{2})$. Then, we have:

$$\min_{i=1,2,\dots,n} \langle \mathbf{v}_i, \mathbf{C}\mathbf{v}_i \rangle_{L^2(p_i)} \leq \frac{1}{n} \sum_{i=1}^n \langle \mathbf{v}_i, \mathbf{C}\mathbf{v}_i \rangle_{L^2(p_i)} \leq \frac{\mathcal{L}(p_0)}{c_\eta n}.$$

The corollary indicates that the gradient norm will converge to zero as n increases. However, similar to the argument mentioned in the continuous-time analysis, it is not guaranteed that it converges to the globally optimal solution because of the non-convexity of \mathcal{L} .

3.2 Particle Approximation of Gradient Flows

In this section, we introduce practical methods for solving problem (8) using the proposed gradient flows (14). To achieve this, it is common to assume that the distribution p is described by a set of variational parameters λ . Specifically, we maintain a set of K particles $\{\lambda_{k,n}\}_{k=1}^K$ for the n -th iteration, and update them in the following manner:

$$\lambda_{k,n+1} = \lambda_{k,n} - \eta \mathbf{C}(\lambda_{k,n}) \nabla \frac{\delta \mathcal{L}}{\delta p_n}(\lambda_{k,n}). \quad (16)$$

We now demonstrate the simplicity of our update (16) when $q(\mathbf{z}|\lambda)$ is a mean-field Gaussian distribution, i.e. $q(\mathbf{z}|\lambda) = \mathcal{N}(\mathbf{z}|\mu, \sigma^2)$.

Gradient flow VI (GFlow-VI). First, we consider the case $\mathbf{C} = \mathbf{I}$. Let $\lambda_{k,n} = (\mu_{k,n}, \mathbf{s}_{k,n})$ be the k -th variational parameter at n -th iteration, where $\mathbf{s}_{k,n} = \sigma_{k,n}^{-2}$ for $k = 1, 2, \dots, K$. Each variational parameter corresponds to a Gaussian distribution, and so we refer it to as "Gaussian particle". For each iteration n , we generate a sample \mathbf{z} from $q(\mathbf{z}|\lambda_{k,n})$. Then we update the mean $\mu_{k,n}$ and the vector $\mathbf{s}_{k,n}$ as follows:

$$\begin{aligned} \mu_{k,n+1} &= \mu_{k,n} - \eta [\nabla_{\mathbf{z}} f(\mathbf{z}) + \nabla_{\mathbf{z}} \log q_n(\mathbf{z})] - \eta \mathbf{w}_k \nabla_{\mu_k} \log q(\mathbf{z}|\lambda_{k,n}). \\ \mathbf{s}_{k,n+1} &= \mathbf{s}_{k,n} - \eta \mathbf{w}_k \nabla_{\mathbf{s}_k} \log q(\mathbf{z}|\lambda_{k,n}) + \frac{\eta}{2} \odot (\mathbf{s}_{k,n} \odot \mathbf{s}_{k,n}) \odot \text{diag} [\nabla_{\mathbf{z}}^2 f(\mathbf{z}) + \nabla_{\mathbf{z}}^2 \log q_n(\mathbf{z})] \end{aligned} \quad (17)$$

where $\mathbf{w}_k = q(\mathbf{z}|\lambda_{k,n})/q_n(\mathbf{z})$, $q_n(\mathbf{z}) = 1/K \sum_{k=1}^K q(\mathbf{z}|\lambda_{k,n})$, and $\mathbf{a} \odot \mathbf{b}$ denotes the element-wise division between vectors \mathbf{a} and \mathbf{b} . We refer to this update as gradient-flow variational inference (GFlow-VI). In fact, the update (17) is obtained using the following relation for a Gaussian distribution $q(\mathbf{z}|\lambda) = N(\mathbf{z}|\mu, \Sigma)$:

$$\begin{aligned} \nabla_{\mu} \mathbb{E}_{\mathbf{z} \sim q(\cdot|\lambda)} [h(\mathbf{z})] &= \mathbb{E}_{\mathbf{z} \sim q(\cdot|\lambda)} [\nabla_{\mathbf{z}} h(\mathbf{z})]. \\ \nabla_{\Sigma} \mathbb{E}_{\mathbf{z} \sim q(\cdot|\lambda)} [h(\mathbf{z})] &= \frac{1}{2} \mathbb{E}_{\mathbf{z} \sim q(\cdot|\lambda)} [\nabla_{\mathbf{z}}^2 h(\mathbf{z})]. \end{aligned} \quad (18)$$

Natural-gradient flow VI (NGFlow-VI). Next, we consider the case that $\mathbf{C} = \mathbf{F}^{-1}$ is the inverse FIM. As much discussed in previous studies, e.g. [9], the natural-gradient update does not require the need of inverting the FIM for

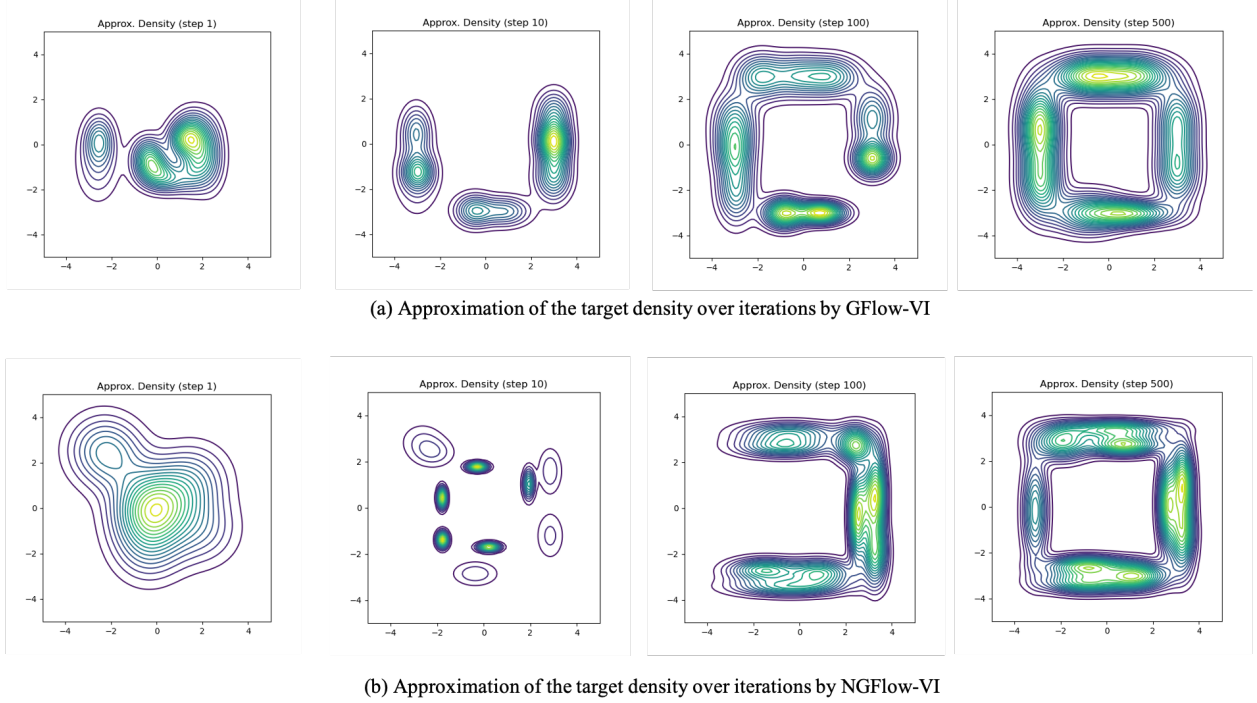


Figure 2: Approximation of the target distribution with 10 Gaussian particles over iterations: 1, 10, 100 and 500. The approximations are estimated by (a) GFlow-VI and (b) NGFlow-VI.

specific types of models and applications, e.g. exponential-family distributions. Thus, in this case, we consider λ to be the natural-parameters of the Gaussian $q(\mathbf{z}|\lambda)$. Specifically, the natural parameters and expectation-parameters can be defined as follows:

$$\lambda_{k,n}^{(1)} = \mathbf{s}_{k,n} \odot \mu_{k,n}, \lambda_{k,n}^{(2)} = -\frac{1}{2}\mathbf{s}_{k,n}$$

and

$$\mathbf{m}_{k,n}^{(1)} = \mu_{k,n}, \mathbf{m}_{k,n}^{(2)} = \mu_{k,n} \odot \mu_{k,n} + 1 \odot \mathbf{s}_{k,n}.$$

The computational efficiency of the natural-gradients is a result of the following relation:

$$\mathbf{F}^{-1}(\lambda_{k,n}) \nabla_{\lambda} \frac{\delta \mathcal{L}}{\delta p_n}(\lambda_{k,n}) = \nabla_{\mathbf{m}} \frac{\delta \mathcal{L}}{\delta p_n}(\lambda_{k,n}). \quad (19)$$

Using the relation (18) and relation in [9], the update (14) in this case can be simplified as follows:

$$\begin{aligned} \mu_{k,n+1} &= \mu_{k,n} - \eta [\nabla_{\mathbf{z}} f(\mathbf{z}) + \nabla_{\mathbf{z}} \log q_n(\mathbf{z})] \odot \mathbf{s}_{k,n+1} - \eta \mathbf{w}_k \nabla_{\mu_k} \log q(\mathbf{z}|\lambda_{k,n}) \odot \mathbf{s}_{k,n+1} \\ \mathbf{s}_{k,n+1} &= \mathbf{s}_{k,n} + \eta \text{diag} [\nabla_{\mathbf{z}}^2 f(\mathbf{z}) + \nabla_{\mathbf{z}}^2 \log q_n(\mathbf{z})] - 2\eta \mathbf{w}_k (\mathbf{s}_{k,n} \odot \mathbf{s}_{k,n}) \odot \nabla_{\mathbf{s}_k} \log q(\mathbf{z}|\lambda_{k,n}) \end{aligned} \quad (20)$$

We refer to this update as natural-gradient flow VI (NGFlow-VI). Detailed derivations of the updates can be found in the supplementary material.

Remark 3. We observe that GFlow-VI and NGFlow-VI serve as extensions of BBVI and NGVI to the cases where the variational distributions take the form of mixtures, where each component is characterized by a Gaussian particle.

3.3 A Simple Fix to Negative Hessian Problem

In the updates (17) and (20), the vectors $\mathbf{s}_{k,n}$ (for $k = 1, 2, \dots, K$) are updated based on the Hessian of $f(\mathbf{z}) + \log q(\mathbf{z})$. However, it is important to note that as $f(\mathbf{z}) + \log q(\mathbf{z})$ is a non-convex function with respect to \mathbf{z} , the Hessian may not be positive-definite, which can lead to method instability. One possible approach to address this issue is to employ the generalized Gaussian-Newton approximation [9] to solve this problem. Unfortunately, we observe that this method does not effectively mitigate the problem when applied to $f(\mathbf{z}) + \log q(\mathbf{z})$.

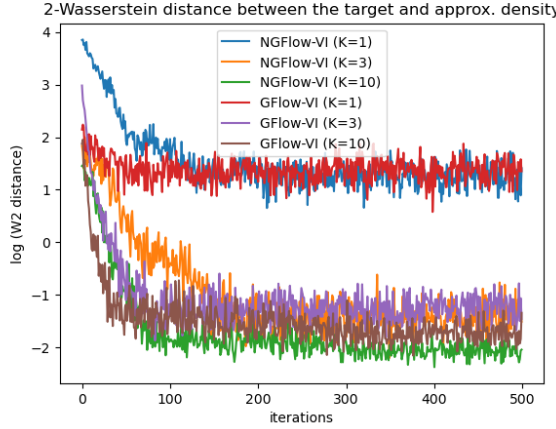


Figure 3: Convergence of two methods GFlow-VI and NGFlow-VI with varying values of K (the number of Gaussian particles): 1, 3 and 10. For each iteration, 2-Wasserstein distance between the approximated density and the target distribution is measured.

In this subsection, we introduce a solution to this issue by using the approach proposed in [12], which involves updating particles within a constrained domain. We observe that in the updates (17) and (20), variance vectors appear independently in the second part of the variational parameters, i.e. $\boldsymbol{\lambda}_{k,n}^{(2)} = \mathbf{s}_{k,n}$ for the first case ($\mathbf{C} = \mathbf{I}$) and $\boldsymbol{\lambda}_{k,n}^{(2)} = -1/2\mathbf{s}_{k,n}$ for the second case ($\mathbf{C} = \mathbf{F}^{-1}$). Thus, it is convenient to turn our problems into the problem of updating particles in the constrained domain, which is already addressed in [12].

We define a strongly convex function φ as follows:

$$\varphi(\boldsymbol{\lambda}) = \frac{1}{2}\|\boldsymbol{\lambda}^{(1)}\|_2^2 + \lambda^{(2)}(\log \boldsymbol{\lambda}^{(2)} - 1).$$

This function is composed of two parts: the first part is to keep the $\boldsymbol{\lambda}^{(1)}$ unchanged while the second part is to handle the non-negative constraint of $\boldsymbol{\lambda}^{(2)}$, which corresponds to the variance (see [2] for the background of the mirror descent). Then the mirror map induced by this convex function φ can be defined as follows:

$$\nabla \varphi(\boldsymbol{\lambda}) = \boldsymbol{\zeta}, \quad (21)$$

where $\boldsymbol{\zeta} \in \mathbb{R}^d$ is defined as: $\boldsymbol{\zeta}^{(1)} = \boldsymbol{\lambda}^{(1)}$ and $\boldsymbol{\zeta}^{(2)} = \log \boldsymbol{\lambda}^{(2)}$. Also the inverse of the mirror map is defined as follows:

$$\nabla \varphi^*(\boldsymbol{\zeta}) = \boldsymbol{\lambda}, \quad (22)$$

where $\boldsymbol{\lambda}^{(1)} = \boldsymbol{\zeta}^{(1)}$, $\boldsymbol{\lambda}^{(2)} = \exp(\boldsymbol{\zeta}^{(2)})$ and φ^* denotes the dual function of φ . The basic idea of our solution is that before each update, we first map the parameters $\boldsymbol{\lambda}_{k,n}$ (for $k = 1, 2, \dots, K$) to the dual space using the mirror map defined by (21) and subsequently update these parameters by the given direction. At the end of each iteration, we map them back to the original space by using the inverse map defined by (22). This proposed updates guarantee that the updated parameters always belong to the constrained domain. In summary, we modify the updates (17) and (20) to fix the negative Hessian problem as follows: For GFlow-VI, we have

$$\begin{aligned} \mathbf{s}'_{k,n} &= \log(\mathbf{s}_{k,n}). \\ \mathbf{s}'_{k,n+1} &= \mathbf{s}'_{k,n} - \eta \mathbf{w}_k \nabla_{\mathbf{s}_k} \log q(\mathbf{z}|\boldsymbol{\lambda}_{k,n}) + \frac{\eta}{2} \odot (\mathbf{s}_{k,n} \odot \mathbf{s}_{k,n}) \odot \text{diag} [\nabla_{\mathbf{z}}^2 f(\mathbf{z}) + \nabla_{\mathbf{z}}^2 \log q_n(\mathbf{z})] \\ \mathbf{s}_{k,n+1} &= \exp(\mathbf{s}'_{k,n+1}). \\ \boldsymbol{\mu}_{k,n+1} &= \boldsymbol{\mu}_{k,n} - \eta [\nabla_{\mathbf{z}} f(\mathbf{z}) + \nabla_{\mathbf{z}} \log q_n(\mathbf{z})] - \eta \mathbf{w}_k \nabla_{\boldsymbol{\mu}_k} \log q(\mathbf{z}|\boldsymbol{\lambda}_{k,n}), \end{aligned} \quad (23)$$

where the first line is to map the vectors $\mathbf{s}_{k,n}$ to the dual space through the mirror map (21), the second line is to update these vectors in the dual space, and the third line is to map the updated variance vectors back to the constrained domain through the inverse map (22). It can be confirmed that the variance vectors are always positive.

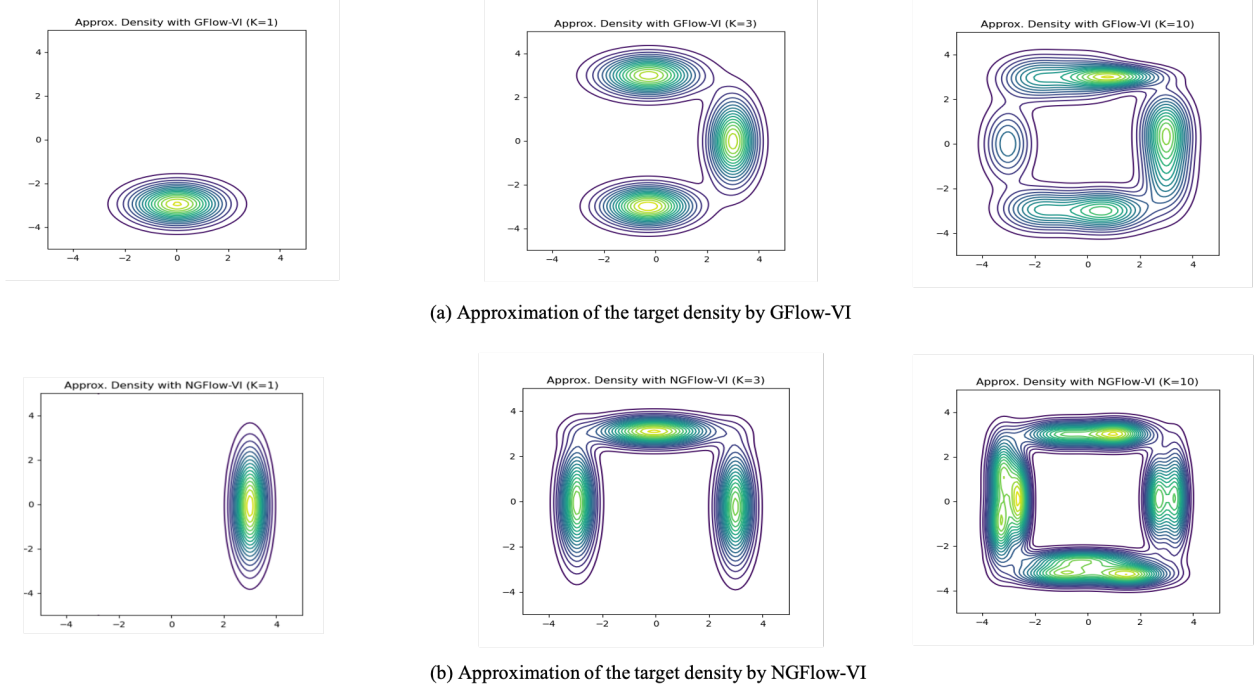


Figure 4: Approximated densities generated by GFlow-VI and NGFlow-VI with varying values of K (the number of Gaussian particles): 1, 3 and 10. (a) approximated densities generated by GFlow-VI, (b) approximated densities generated by NGFlow-VI.

For NGFlow-VI, we apply the same procedure to update the variance vectors. The modification of the update (20) can be expressed as follows:

$$\begin{aligned}
 \mathbf{s}'_{k,n} &= \log(\mathbf{s}_{k,n}). \\
 \mathbf{s}'_{k,n+1} &= \mathbf{s}'_{k,n} + \eta \text{diag} [\nabla_{\mathbf{z}}^2 f(\mathbf{z}) + \nabla_{\mathbf{z}}^2 \log q_n(\mathbf{z})] - 2\eta \mathbf{w}_k (\mathbf{s}_{k,n} \odot \mathbf{s}_{k,n}) \odot \nabla_{\mathbf{s}_k} \log q(\mathbf{z}|\lambda_{k,n}). \\
 \mathbf{s}_{k,n+1} &= \exp(\mathbf{s}'_{k,n+1}). \\
 \boldsymbol{\mu}_{k,n+1} &= \boldsymbol{\mu}_{k,n} - \eta [\nabla_{\mathbf{z}} f(\mathbf{z}) + \nabla_{\mathbf{z}} \log q_n(\mathbf{z})] \odot \mathbf{s}_{k,n+1} - \eta \mathbf{w}_k \nabla_{\boldsymbol{\mu}_k} \log q(\mathbf{z}|\lambda_{k,n}) \odot \mathbf{s}_{k,n+1}.
 \end{aligned} \tag{24}$$

4 Numerical Experiments

In this section, we perform a series of experiments to validate and enhance our theoretical analyses. Our focus is on a mixture of four Gaussian distributions, which serves as the target distribution (as shown in Figure 1): for any $\mathbf{z} \in \mathbb{R}^2$,

$$\pi(\mathbf{z}) =$$

$$\frac{1}{4} \mathcal{N} \left(\mathbf{z} \left| \begin{bmatrix} 0 \\ 3 \end{bmatrix}, \begin{bmatrix} 0.5 & 0 \\ 0 & 6 \end{bmatrix} \right. \right) + \frac{1}{4} \mathcal{N} \left(\mathbf{z} \left| \begin{bmatrix} 0 \\ -3 \end{bmatrix}, \begin{bmatrix} 0.5 & 0 \\ 0 & 6 \end{bmatrix} \right. \right) + \frac{1}{4} \mathcal{N} \left(\mathbf{z} \left| \begin{bmatrix} 3 \\ 0 \end{bmatrix}, \begin{bmatrix} 6 & 0 \\ 0 & 0.5 \end{bmatrix} \right. \right) + \frac{1}{4} \mathcal{N} \left(\mathbf{z} \left| \begin{bmatrix} -3 \\ 0 \end{bmatrix}, \begin{bmatrix} 6 & 0 \\ 0 & 0.5 \end{bmatrix} \right. \right)$$

We conduct a comparative analysis of GFlow-VI and NGFlow-VI using different numbers of Gaussian particles, i.e. K , to approximate the target distribution π . As mentioned earlier, when the number of particles, K , is set to 1, the updates of GFlow-VI and NGFlow-VI reduce to those of BBVI and NGVI, respectively.

Initially, the mean $\boldsymbol{\mu}_{k,0}$ of each Gaussian particle is randomly sampled from a 2D normal distribution, i.e. $\boldsymbol{\mu}_{k,0} \sim \mathcal{N}(0, \mathbf{I})$. The variance vector of each particle is initialized as one (the identity matrix). Subsequently, the mean vectors and variance vectors of Gaussian particles are updated by 500 iterations of GFlow-VI and NGFlow-VI, employing a fixed learning rate of 0.01. The number of samples to estimate the expectation $\mathbb{E}_{\mathbf{z} \sim q(\cdot|\lambda)}[\cdot]$ is set to 1.

Figure 2 shows the contour-line representations of the approximated density compared to the target distribution for iterations 1, 10, 100 and 500. These updates are performed using GFlow-VI (Figure 2a) and NGFlow-VI (Figure 2b). Notably, the figures illustrate how the Gaussian particles gradually become more diverse, covering all modes of the target distribution as the iterations progress.

Next we consider the performance of GFlow-VI and NGFlow-VI with varying values of K (the number of Gaussian particles): 1, 3 and 10. We compare the methods by measuring the 2-Wasserstein distance between the target distribution and the approximated densities given by the compared methods. To achieve this, we generate 500 samples for both the approximated density and the target distribution and calculate the 2-Wasserstein distance using the POT library [5]. Figure 3 shows the convergence behavior of GFlow-VI and NGFlow-VI under different values of K . Notably, when $K = 1$, corresponding to BBVI and NGVI, both methods yields poor approximations since a single Gaussian particle might fail to effectively capture the multi-modal target distribution. However, when $K = 10$, both methods excel in approximating the target distribution effectively.

We further look into the approximated densities generated by the two updates GFlow-VI and NGFlow-VI. As shown in Figure 4, an interesting observation emerges. When $K = 1$, the approximated densities only encompass a single mode of the target distribution, resulting in a relatively poor approximation. However, when we increase the value of K to 3, the approximated densities are improved significantly, now covering three modes of the target distribution. The best approximation is achieved when $K = 10$, where the approximated densities span all the modes. These suggest that when the number of Gaussian particles is large, both of these updates can approximate more complicated target distributions. Nonetheless, it is noteworthy that it also increases the computational complexity due to the increased number of Gaussian particles.

5 Conclusions

We have presented a novel approach based on the Wasserstein gradient flows for solving VI. The distinction of our approach lies on the definition of the domain: while the previous methods define the Wasserstein gradient flows over the domains of latent variables, our approach define them on the domains of variational parameters of VI. This distinction allows our approach to convey significant novel contributions to the relevant fields. Based on the established theories for the defined gradient flows, we also presented the particle-based algorithms for VI and show the effectiveness of the proposed algorithm through empirical experiments on the synthetic data.

The proposed updates, GFlow-VI and NGFlow-VI, have a common fixed weight restriction. This restriction implies that weights of all Gaussian particles remain constant throughout the optimization process, while only particle positions are updated. This restriction might limit the approximation capacity of the variational distribution, especially when the number of Gaussian particles, K , is limited. To address this limitation, possible future work would be to explore the use of Wasserstein-Fisher-Rao gradient flows [6], which allow the simultaneous update of both positions and weights of Gaussian particles.

References

- [1] Shun-Ichi Amari and Scott C Douglas. Why natural gradient? In *Proceedings of the 1998 IEEE International Conference on Acoustics, Speech and Signal Processing, ICASSP'98 (Cat. No. 98CH36181)*, volume 2, pages 1213–1216. IEEE, 1998.
- [2] Amir Beck and Marc Teboulle. Mirror descent and nonlinear projected subgradient methods for convex optimization. *Operations Research Letters*, 31(3):167–175, 2003.
- [3] David M Blei, Alp Kucukelbir, and Jon D McAuliffe. Variational inference: A review for statisticians. *Journal of the American statistical Association*, 112(518):859–877, 2017.
- [4] Aaron M Ellison. Bayesian inference in ecology. *Ecology letters*, 7(6):509–520, 2004.
- [5] Rémi Flamary, Nicolas Courty, Alexandre Gramfort, Mokhtar Z Alaya, Aurélie Boisbunon, Stanislas Chambon, Laetitia Chapel, Adrien Corenflos, Kilian Fatras, Nemo Fournier, et al. Pot: Python optimal transport. *The Journal of Machine Learning Research*, 22(1):3571–3578, 2021.
- [6] Thomas O Gallouët and Leonard Monsaingeon. A jko splitting scheme for kantorovich–fisher–rao gradient flows. *SIAM Journal on Mathematical Analysis*, 49(2):1100–1130, 2017.
- [7] Michael I Jordan, Zoubin Ghahramani, Tommi S Jaakkola, and Lawrence K Saul. An introduction to variational methods for graphical models. *Machine learning*, 37:183–233, 1999.
- [8] Richard Jordan, David Kinderlehrer, and Felix Otto. The variational formulation of the fokker–planck equation. *SIAM journal on mathematical analysis*, 29(1):1–17, 1998.
- [9] Mohammad Emtiyaz Khan and Didrik Nielsen. Fast yet simple natural-gradient descent for variational inference in complex models. In *2018 International Symposium on Information Theory and Its Applications (ISITA)*, pages 31–35. IEEE, 2018.

- [10] Marc Lambert, Sinho Chewi, Francis Bach, Silvère Bonnabel, and Philippe Rigollet. Variational inference via wasserstein gradient flows. *Advances in Neural Information Processing Systems*, 35:14434–14447, 2022.
- [11] Dennis Victor Lindley. *Bayesian statistics: A review*. SIAM, 1972.
- [12] Dai Hai Nguyen and Tetsuya Sakurai. Mirror variational transport: a particle-based algorithm for distributional optimization on constrained domains. *Machine Learning*, 112(8):2845–2869, 2023.
- [13] Dai Hai Nguyen and Koji Tsuda. On a linear fused gromov-wasserstein distance for graph structured data. *Pattern Recognition*, 138:109351, 2023.
- [14] Dai Hai Nguyen, Canh Hao Nguyen, and Hiroshi Mamitsuka. Learning subtree pattern importance for weisfeiler-lehman based graph kernels. *Machine Learning*, 110:1585–1607, 2021.
- [15] Hermina Petric Maretic, Mireille El Gheche, Giovanni Chierchia, and Pascal Frossard. Got: an optimal transport framework for graph comparison. *Advances in Neural Information Processing Systems*, 32, 2019.
- [16] Rajesh Ranganath, Sean Gerrish, and David Blei. Black box variational inference. In *Artificial intelligence and statistics*, pages 814–822. PMLR, 2014.
- [17] Filippo Santambrogio. Optimal transport for applied mathematicians. *Birkhäuser, NY*, 55(58-63):94, 2015.
- [18] Udo Von Toussaint. Bayesian inference in physics. *Reviews of Modern Physics*, 83(3):943, 2011.
- [19] Rentian Yao and Yun Yang. Mean field variational inference via wasserstein gradient flow. *arXiv preprint arXiv:2207.08074*, 2022.
- [20] Cheng Zhang, Judith Bütepage, Hedvig Kjellström, and Stephan Mandt. Advances in variational inference. *IEEE transactions on pattern analysis and machine intelligence*, 41(8):2008–2026, 2018.

A Supplementary Materials of Wasserstein Gradient Flow over Variational Parameter Space for Variational Inference

A.1 Proof of Theorem 1

Proof. To compute the first variation of $\mathcal{L}(p)$, suppose that $\varepsilon > 0$ and an arbitrary distribution $\chi \in \mathcal{P}(\Omega)$. We compute $(\mathcal{L}(p + \varepsilon\chi) - \mathcal{L}(p))/\varepsilon$ as follows:

$$\begin{aligned}
& \frac{1}{\varepsilon} [\mathcal{L}(p + \varepsilon\chi) - \mathcal{L}(p)] = \\
& \frac{1}{\varepsilon} \int_{\boldsymbol{\lambda}} (p(\boldsymbol{\lambda}) + \varepsilon\chi(\boldsymbol{\lambda})) \int_{\mathbf{z}} q(\mathbf{z}|\boldsymbol{\lambda}) \left[f(\mathbf{z}) + \log \left(\int_{\boldsymbol{\lambda}} (p(\boldsymbol{\lambda}) + \varepsilon\chi(\boldsymbol{\lambda})) q(\mathbf{z}|\boldsymbol{\lambda}) d\boldsymbol{\lambda} \right) \right] d\mathbf{z} d\boldsymbol{\lambda} \\
& - \frac{1}{\varepsilon} \int_{\boldsymbol{\lambda}} p(\boldsymbol{\lambda}) \int_{\mathbf{z}} q(\mathbf{z}|\boldsymbol{\lambda}) \left[f(\mathbf{z}) + \log \left(\int_{\boldsymbol{\lambda}} p(\boldsymbol{\lambda}) q(\mathbf{z}|\boldsymbol{\lambda}) d\boldsymbol{\lambda} \right) \right] d\mathbf{z} d\boldsymbol{\lambda} \\
& = \int_{\boldsymbol{\lambda}} \chi(\boldsymbol{\lambda}) \int_{\mathbf{z}} q(\mathbf{z}|\boldsymbol{\lambda}) f(\mathbf{z}) d\mathbf{z} d\boldsymbol{\lambda} + \frac{1}{\varepsilon} \int_{\boldsymbol{\lambda}} (p(\boldsymbol{\lambda}) + \varepsilon\chi(\boldsymbol{\lambda})) \int_{\mathbf{z}} q(\mathbf{z}|\boldsymbol{\lambda}) \log \left(\int_{\boldsymbol{\lambda}} (p(\boldsymbol{\lambda}) + \varepsilon\chi(\boldsymbol{\lambda})) q(\mathbf{z}|\boldsymbol{\lambda}) d\boldsymbol{\lambda} \right) d\mathbf{z} d\boldsymbol{\lambda} \\
& - \frac{1}{\varepsilon} \int_{\boldsymbol{\lambda}} p(\boldsymbol{\lambda}) \int_{\mathbf{z}} q(\mathbf{z}|\boldsymbol{\lambda}) \log \left(\int_{\boldsymbol{\lambda}} p(\boldsymbol{\lambda}) q(\mathbf{z}|\boldsymbol{\lambda}) d\boldsymbol{\lambda} \right) d\mathbf{z} d\boldsymbol{\lambda} \\
& = \int_{\boldsymbol{\lambda}} \chi(\boldsymbol{\lambda}) \int_{\mathbf{z}} q(\mathbf{z}|\boldsymbol{\lambda}) f(\mathbf{z}) d\mathbf{z} d\boldsymbol{\lambda} \\
& + \frac{1}{\varepsilon} \int_{\boldsymbol{\lambda}} (p(\boldsymbol{\lambda}) + \varepsilon\chi(\boldsymbol{\lambda})) \int_{\mathbf{z}} q(\mathbf{z}|\boldsymbol{\lambda}) \log \left(\int_{\boldsymbol{\lambda}} (p(\boldsymbol{\lambda}) + \varepsilon\chi(\boldsymbol{\lambda})) q(\mathbf{z}|\boldsymbol{\lambda}) d\boldsymbol{\lambda} \right) d\mathbf{z} d\boldsymbol{\lambda} - \\
& \frac{1}{\varepsilon} \int_{\boldsymbol{\lambda}} p(\boldsymbol{\lambda}) \int_{\mathbf{z}} q(\mathbf{z}|\boldsymbol{\lambda}) \log \left(\int_{\boldsymbol{\lambda}} (p(\boldsymbol{\lambda}) + \varepsilon\chi(\boldsymbol{\lambda})) q(\mathbf{z}|\boldsymbol{\lambda}) d\boldsymbol{\lambda} \right) d\mathbf{z} d\boldsymbol{\lambda} \\
& + \frac{1}{\varepsilon} \left[\int_{\boldsymbol{\lambda}} p(\boldsymbol{\lambda}) \int_{\mathbf{z}} q(\mathbf{z}|\boldsymbol{\lambda}) \log \left(\int_{\boldsymbol{\lambda}} (p(\boldsymbol{\lambda}) + \varepsilon\chi(\boldsymbol{\lambda})) q(\mathbf{z}|\boldsymbol{\lambda}) d\boldsymbol{\lambda} \right) d\mathbf{z} d\boldsymbol{\lambda} - \int_{\boldsymbol{\lambda}} p(\boldsymbol{\lambda}) \int_{\mathbf{z}} q(\mathbf{z}|\boldsymbol{\lambda}) \log \left(\int_{\boldsymbol{\lambda}} p(\boldsymbol{\lambda}) q(\mathbf{z}|\boldsymbol{\lambda}) d\boldsymbol{\lambda} \right) d\mathbf{z} d\boldsymbol{\lambda} \right] \\
& = \int_{\boldsymbol{\lambda}} \chi(\boldsymbol{\lambda}) \int_{\mathbf{z}} q(\mathbf{z}|\boldsymbol{\lambda}) f(\mathbf{z}) d\mathbf{z} d\boldsymbol{\lambda} \\
& + \underbrace{\int_{\boldsymbol{\lambda}} \chi(\boldsymbol{\lambda}) \int_{\mathbf{z}} q(\mathbf{z}|\boldsymbol{\lambda}) \log \left(\int_{\boldsymbol{\lambda}} (p(\boldsymbol{\lambda}) + \varepsilon\chi(\boldsymbol{\lambda})) q(\mathbf{z}|\boldsymbol{\lambda}) d\boldsymbol{\lambda} \right) d\mathbf{z} d\boldsymbol{\lambda}}_{(a)} \\
& + \underbrace{\frac{1}{\varepsilon} \left[\int_{\boldsymbol{\lambda}} p(\boldsymbol{\lambda}) \int_{\mathbf{z}} q(\mathbf{z}|\boldsymbol{\lambda}) \log \left(1 + \frac{\varepsilon \int_{\boldsymbol{\lambda}} \chi(\boldsymbol{\lambda}) q(\mathbf{z}|\boldsymbol{\lambda}) d\boldsymbol{\lambda}}{\int_{\boldsymbol{\lambda}} p(\boldsymbol{\lambda}) q(\mathbf{z}|\boldsymbol{\lambda}) d\boldsymbol{\lambda}} \right) d\mathbf{z} d\boldsymbol{\lambda} \right]}_{(b)}
\end{aligned}$$

We process parts (a) and (b), when $\varepsilon \rightarrow 0$, as follows:

$$\begin{aligned}
\lim_{\varepsilon \rightarrow 0} (a) &= \int_{\boldsymbol{\lambda}} \chi(\boldsymbol{\lambda}) \int_{\mathbf{z}} q(\mathbf{z}|\boldsymbol{\lambda}) \log \left(\int_{\boldsymbol{\lambda}} p(\boldsymbol{\lambda}) q(\mathbf{z}|\boldsymbol{\lambda}) d\boldsymbol{\lambda} \right) d\mathbf{z} d\boldsymbol{\lambda} \\
\lim_{\varepsilon \rightarrow 0} (b) &= \int_{\boldsymbol{\lambda}} p(\boldsymbol{\lambda}) \int_{\mathbf{z}} q(\mathbf{z}|\boldsymbol{\lambda}) \frac{\int_{\boldsymbol{\lambda}} \chi(\boldsymbol{\lambda}) q(\mathbf{z}|\boldsymbol{\lambda}) d\boldsymbol{\lambda}}{\int_{\boldsymbol{\lambda}} p(\boldsymbol{\lambda}) q(\mathbf{z}|\boldsymbol{\lambda}) d\boldsymbol{\lambda}} d\mathbf{z} d\boldsymbol{\lambda} = \int_{\mathbf{z}} \int_{\boldsymbol{\lambda}} p(\boldsymbol{\lambda}) q(\mathbf{z}|\boldsymbol{\lambda}) d\boldsymbol{\lambda} \frac{\int_{\boldsymbol{\lambda}} \chi(\boldsymbol{\lambda}) q(\mathbf{z}|\boldsymbol{\lambda}) d\boldsymbol{\lambda}}{\int_{\boldsymbol{\lambda}} p(\boldsymbol{\lambda}) q(\mathbf{z}|\boldsymbol{\lambda}) d\boldsymbol{\lambda}} d\mathbf{z} \\
&= \int_{\boldsymbol{\lambda}} \chi(\boldsymbol{\lambda}) \int_{\mathbf{z}} q(\mathbf{z}|\boldsymbol{\lambda}) d\mathbf{z} d\boldsymbol{\lambda} = \int_{\boldsymbol{\lambda}} \chi(\boldsymbol{\lambda}) d\boldsymbol{\lambda}
\end{aligned}$$

where we have used the following equality for (b): $\lim_{\varepsilon \rightarrow 0} \frac{\log(1+\varepsilon x)}{\varepsilon} = x$ for all $x \in \mathbb{R}$.

So, we have:

$$\lim_{\varepsilon \rightarrow 0} \frac{1}{\varepsilon} [\mathcal{L}(p + \varepsilon\chi) - \mathcal{L}(p)] = \int_{\boldsymbol{\lambda}} \chi(\boldsymbol{\lambda}) (\mathbb{E}_{\mathbf{z} \sim q(\cdot|\boldsymbol{\lambda})} [f(\mathbf{z}) + \log q(\mathbf{z})] + 1) d\boldsymbol{\lambda}$$

By definition of the first variation of \mathcal{L} , this completes the proof. \square

A.2 Proof of Proposition 3

Proof. Denote $\mathbf{v}_n(\boldsymbol{\lambda}) = -\nabla_{\boldsymbol{\lambda}} \mathbb{E}_{\mathbf{z} \sim q(\cdot | \boldsymbol{\lambda})} [f(\mathbf{z}) + \log q_n(\mathbf{z})]$ where $q_n(\mathbf{z}) = \mathbb{E}_{\boldsymbol{\lambda} \sim p_n} [q(\mathbf{z} | \boldsymbol{\lambda})]$, $\Phi_t(\boldsymbol{\lambda}) = \boldsymbol{\lambda} + t\mathbf{C}(\boldsymbol{\lambda})\mathbf{v}_n(\boldsymbol{\lambda})$ for $t \in [0, \eta]$, and $\rho_t = (\Phi_t)_{\#} p_n$. Then it is evident that $\rho_0 = p_n$ and $\rho_{\eta} = p_{n+1}$.

We define $\phi(t) = \mathcal{L}(\rho_t)$. Clearly, $\phi(0) = \mathcal{L}(p_n)$ and $\phi(\eta) = \mathcal{L}(p_{n+1})$. Using a Taylor expansion, we have:

$$\phi(\eta) = \phi(0) + \eta\phi'(0) + \int_0^{\eta} (\eta - t)\phi''(t)dt \quad (25)$$

Using the chain rule, we can estimate $\phi'(t)$ as follows:

$$\begin{aligned} \phi'(t) &= \frac{d}{dt} \int_{\boldsymbol{\lambda}} \rho_t(\boldsymbol{\lambda}) \int_{\mathbf{z}} q(\mathbf{z} | \boldsymbol{\lambda}) \left[f(\mathbf{z}) + \log \left(\int_{\boldsymbol{\lambda}} \rho_t(\boldsymbol{\lambda}) q(\mathbf{z} | \boldsymbol{\lambda}) \right) \right] d\mathbf{z} d\boldsymbol{\lambda} \\ &= \frac{d}{dt} \int_{\boldsymbol{\lambda}} p_n(\boldsymbol{\lambda}) \int_{\mathbf{z}} q(\mathbf{z} | \Phi_t(\boldsymbol{\lambda})) \left[f(\mathbf{z}) + \log \left(\int_{\boldsymbol{\lambda}} p_n(\boldsymbol{\lambda}) q(\mathbf{z} | \Phi_t(\boldsymbol{\lambda})) \right) \right] d\mathbf{z} d\boldsymbol{\lambda} \\ &= \int_{\boldsymbol{\lambda}} p_n(\boldsymbol{\lambda}) \left\langle \frac{d\Phi_t(\boldsymbol{\lambda})}{dt}, \nabla_{\boldsymbol{\lambda}} \int_{\mathbf{z}} q(\mathbf{z} | \Phi_t(\boldsymbol{\lambda})) \left[f(\mathbf{z}) + \log \left(\int_{\boldsymbol{\lambda}} p_n(\boldsymbol{\lambda}) q(\mathbf{z} | \Phi_t(\boldsymbol{\lambda})) \right) \right] d\mathbf{z} \right\rangle d\boldsymbol{\lambda} \\ &= \int_{\boldsymbol{\lambda}} p_n(\boldsymbol{\lambda}) \langle \mathbf{C}(\boldsymbol{\lambda})\mathbf{v}_n(\boldsymbol{\lambda}), \nabla_{\boldsymbol{\lambda}} \mathbb{E}_{\mathbf{z} \sim q(\cdot | \Phi_t(\boldsymbol{\lambda}))} [f(\mathbf{z}) + \log q_t(\mathbf{z})] \rangle d\boldsymbol{\lambda}, \end{aligned}$$

where $q_t(\mathbf{z}) = \int_{\boldsymbol{\lambda}} p_n(\boldsymbol{\lambda}) q(\mathbf{z} | \Phi_t(\boldsymbol{\lambda})) d\boldsymbol{\lambda}$. The second equality is obtained by applying the change of variable formula, and the last equality is obtained by the definition of \mathbf{v}_n and Φ_t .

So, at $t = 0$, we have:

$$\phi'(0) = - \int_{\boldsymbol{\lambda}} \langle \mathbf{v}_n(\boldsymbol{\lambda}), \mathbf{C}(\boldsymbol{\lambda})\mathbf{v}_n(\boldsymbol{\lambda}) \rangle p_n(\boldsymbol{\lambda}) d\boldsymbol{\lambda} = -\langle \mathbf{v}_n, \mathbf{C}\mathbf{v}_n \rangle_{L^2(p_n)} \quad (26)$$

Next we estimate $\phi''(\boldsymbol{\lambda})$ as follows:

$$\begin{aligned} \phi''(\boldsymbol{\lambda}) &= \frac{d}{dt} \phi'(t) = \int_{\boldsymbol{\lambda}} p_n(\boldsymbol{\lambda}) \langle \mathbf{C}(\boldsymbol{\lambda})\mathbf{v}_n(\boldsymbol{\lambda}), \frac{d}{dt} \nabla_{\boldsymbol{\lambda}} \mathbb{E}_{\mathbf{z} \sim q(\cdot | \Phi_t(\boldsymbol{\lambda}))} [f(\mathbf{z}) + \log q_t(\mathbf{z})] \rangle d\boldsymbol{\lambda} \\ &= \int_{\boldsymbol{\lambda}} p_n(\boldsymbol{\lambda}) \langle \mathbf{C}(\boldsymbol{\lambda})\mathbf{v}_n(\boldsymbol{\lambda}), \mathbf{H}_t(\boldsymbol{\lambda})\mathbf{v}_n(\boldsymbol{\lambda}) \rangle d\boldsymbol{\lambda} = \langle \mathbf{C}\mathbf{v}_n, \mathbf{H}_t\mathbf{v}_n \rangle_{L^2(p_n)}, \end{aligned}$$

where $\mathbf{H}_t(\boldsymbol{\lambda}) = \nabla_{\boldsymbol{\lambda}}^2 \mathbb{E}_{\mathbf{z} \sim q(\cdot | \Phi_t(\boldsymbol{\lambda}))} [f(\mathbf{z}) + \log q_t(\mathbf{z})]$. Now we need to upper-bound the operator norm of \mathbf{H}_t .

Denote $\boldsymbol{\lambda}_t = \Phi_t(\boldsymbol{\lambda})$, we can rewrite \mathbf{H}_t as follows:

$$\begin{aligned} \mathbf{H}_t(\boldsymbol{\lambda}) &= \nabla_{\boldsymbol{\lambda}} \left[\int_{\mathbf{z}} \nabla_{\boldsymbol{\lambda}} q(\mathbf{z} | \boldsymbol{\lambda}_t) [f(\mathbf{z}) + \log q_t(\mathbf{z})] d\mathbf{z} + \int_{\mathbf{z}} q(\mathbf{z} | \boldsymbol{\lambda}_t) \nabla_{\boldsymbol{\lambda}} \log q_t(\mathbf{z}) d\mathbf{z} \right] \\ &= \int_{\mathbf{z}} \nabla_{\boldsymbol{\lambda}}^2 q(\mathbf{z} | \boldsymbol{\lambda}_t) [f(\mathbf{z}) + \log q_t(\mathbf{z})] d\mathbf{z} + 2 \int_{\mathbf{z}} [\nabla_{\boldsymbol{\lambda}} q(\mathbf{z} | \boldsymbol{\lambda}_t)] [\nabla_{\boldsymbol{\lambda}} \log q_t(\mathbf{z})]^T d\mathbf{z} + \int_{\mathbf{z}} q(\mathbf{z} | \boldsymbol{\lambda}_t) \nabla_{\boldsymbol{\lambda}}^2 \log q_t(\mathbf{z}) d\mathbf{z} \\ &= \underbrace{\int_{\mathbf{z}} \nabla_{\boldsymbol{\lambda}}^2 q(\mathbf{z} | \boldsymbol{\lambda}_t) [f(\mathbf{z}) + \log q_t(\mathbf{z})] d\mathbf{z}}_{(a)} + 2 \underbrace{\int_{\mathbf{z}} q(\mathbf{z} | \boldsymbol{\lambda}_t) [\nabla_{\boldsymbol{\lambda}} \log q(\mathbf{z} | \boldsymbol{\lambda}_t)] [\nabla_{\boldsymbol{\lambda}} \log q_t(\mathbf{z})]^T d\mathbf{z}}_{(b)} + \underbrace{\int_{\mathbf{z}} q(\mathbf{z} | \boldsymbol{\lambda}_t) \nabla_{\boldsymbol{\lambda}}^2 \log q_t(\mathbf{z}) d\mathbf{z}}_{(c)}, \end{aligned}$$

where the third equality is obtained using the following identity: $\nabla_{\boldsymbol{\lambda}} q(\mathbf{z} | \boldsymbol{\lambda}) = q(\mathbf{z} | \boldsymbol{\lambda}) \nabla_{\boldsymbol{\lambda}} \log q(\mathbf{z} | \boldsymbol{\lambda})$. We process part (a) as follows:

$$\begin{aligned} (a) &= \int_{\boldsymbol{\lambda}} \nabla_{\boldsymbol{\lambda}} [q(\mathbf{z} | \boldsymbol{\lambda}_t) \nabla_{\boldsymbol{\lambda}} \log q(\mathbf{z} | \boldsymbol{\lambda}_t)] [f(\mathbf{z}) + \log q_t(\mathbf{z})] d\boldsymbol{\lambda} \\ &= \int_{\mathbf{z}} \nabla_{\boldsymbol{\lambda}} q(\mathbf{z} | \boldsymbol{\lambda}_t) \nabla_{\boldsymbol{\lambda}} \log q(\mathbf{z} | \boldsymbol{\lambda}_t) [f(\mathbf{z}) + \log q_t(\mathbf{z})] d\mathbf{z} + \int_{\mathbf{z}} q(\mathbf{z} | \boldsymbol{\lambda}_t) \nabla_{\boldsymbol{\lambda}}^2 \log q(\mathbf{z} | \boldsymbol{\lambda}_t) [f(\mathbf{z}) + \log q_t(\mathbf{z})] d\mathbf{z} \\ &= \int_{\mathbf{z}} [\nabla_{\boldsymbol{\lambda}} q(\mathbf{z} | \boldsymbol{\lambda}_t)] [\nabla_{\boldsymbol{\lambda}} \log q(\mathbf{z} | \boldsymbol{\lambda}_t)]^T [f(\mathbf{z}) + \log q_t(\mathbf{z})] d\mathbf{z} + \int_{\mathbf{z}} q(\mathbf{z} | \boldsymbol{\lambda}_t) \nabla_{\boldsymbol{\lambda}}^2 \log q(\mathbf{z} | \boldsymbol{\lambda}_t) [f(\mathbf{z}) + \log q_t(\mathbf{z})] d\mathbf{z} \\ &= \int_{\mathbf{z}} q(\mathbf{z} | \boldsymbol{\lambda}_t) [\nabla_{\boldsymbol{\lambda}} \log q(\mathbf{z} | \boldsymbol{\lambda}_t)] [\nabla_{\boldsymbol{\lambda}} \log q(\mathbf{z} | \boldsymbol{\lambda}_t)]^T [f(\mathbf{z}) + \log q_t(\mathbf{z})] d\mathbf{z} + \int_{\mathbf{z}} q(\mathbf{z} | \boldsymbol{\lambda}_t) \nabla_{\boldsymbol{\lambda}}^2 \log q(\mathbf{z} | \boldsymbol{\lambda}_t) [f(\mathbf{z}) + \log q_t(\mathbf{z})] d\mathbf{z} \end{aligned}$$

The operator norm of part (a) can be upper-bounded as follows:

$$\begin{aligned}
\|(\mathbf{a})\|_{\text{op}} &\leq \mathbb{E}_{\mathbf{z} \sim q(\cdot | \boldsymbol{\lambda}_t)} \|\nabla_{\boldsymbol{\lambda}} \log q(\mathbf{z} | \boldsymbol{\lambda}_t)\|_2^2 |f(\mathbf{z})| + \mathbb{E}_{\mathbf{z} \sim q(\cdot | \boldsymbol{\lambda}_t)} \|\nabla_{\boldsymbol{\lambda}}^2 \log q(\mathbf{z} | \boldsymbol{\lambda}_t)\|_{\text{op}} |f(\mathbf{z})| + \log q_t(\mathbf{z})| \\
&\leq [\mathbb{E}_{\mathbf{z} \sim q(\cdot | \boldsymbol{\lambda}_t)} \|\nabla_{\boldsymbol{\lambda}} \log q(\mathbf{z} | \boldsymbol{\lambda}_t)\|_2^2] [\mathbb{E}_{\mathbf{z} \sim q(\cdot | \boldsymbol{\lambda}_t)} |f(\mathbf{z})| + \mathbb{E}_{\mathbf{z} \sim q(\cdot | \boldsymbol{\lambda}_t)} |\log q_t(\mathbf{z})|] \\
&+ [\mathbb{E}_{\mathbf{z} \sim q(\cdot | \boldsymbol{\lambda}_t)} \|\nabla_{\boldsymbol{\lambda}}^2 \log q(\mathbf{z} | \boldsymbol{\lambda}_t)\|_{\text{op}}] [\mathbb{E}_{\mathbf{z} \sim q(\cdot | \boldsymbol{\lambda}_t)} |f(\mathbf{z})| + \mathbb{E}_{\mathbf{z} \sim q(\cdot | \boldsymbol{\lambda}_t)} |\log q_t(\mathbf{z})|] \\
&\leq (\alpha_1 + \beta_2)(M_1 + M_2),
\end{aligned} \tag{27}$$

where the first inequality is obtained using the equality $\|\mathbf{a}\mathbf{b}^T\|_{\text{op}} = \|\mathbf{a}\|_2 \|\mathbf{b}\|_2$ for two vectors \mathbf{a} and \mathbf{b} ; the second inequality is obtained by using the inequality $\mathbb{E}_{\mathbf{z} \sim q(\cdot | \boldsymbol{\lambda})} |h_1(\mathbf{z})| |h_2(\mathbf{z})| \leq \mathbb{E}_{\mathbf{z} \sim q(\cdot | \boldsymbol{\lambda})} |h_1(\mathbf{z})| \mathbb{E}_{\mathbf{z} \sim q(\cdot | \boldsymbol{\lambda})} |h_2(\mathbf{z})|$ for two scalar functions h_1 and h_2 ; the last inequality is obtained by using assumptions (A1), (A2) and (A3).

Next, the operator norm of part (b) can be upper-bounded as follows:

$$\begin{aligned}
\|(\mathbf{b})\|_{\text{op}} &= 2\mathbb{E}_{\mathbf{z} \sim q(\cdot | \boldsymbol{\lambda}_t)} \|\nabla_{\boldsymbol{\lambda}} \log q(\mathbf{z} | \boldsymbol{\lambda}_t)\|_2 \|\nabla_{\boldsymbol{\lambda}} \log q_t(\mathbf{z})\|_2 \leq \mathbb{E}_{\mathbf{z} \sim q(\cdot | \boldsymbol{\lambda}_t)} \|\nabla_{\boldsymbol{\lambda}} \log q(\mathbf{z} | \boldsymbol{\lambda}_t)\|_2^2 + \mathbb{E}_{\mathbf{z} \sim q(\cdot | \boldsymbol{\lambda}_t)} \|\nabla_{\boldsymbol{\lambda}} \log q(\mathbf{z} | \boldsymbol{\lambda}_t)\|_2^2 \\
&\leq \alpha_1 + \alpha_2,
\end{aligned} \tag{28}$$

where the last inequality is obtained by using assumption (A1).

Putting it all together (27), (28) and assumption A(2) (for upper-bounding part (c)), the operator norm of \mathbf{H}_t can be upper-bounded as follows:

$$\|\mathbf{H}_t(\boldsymbol{\lambda})\|_{\text{op}} \leq (\alpha_1 + \beta_1)(M_1 + M_2) + \alpha_1 + \alpha_2 + \beta_2 = \kappa \tag{29}$$

Thus, plugging the results (26) and (29) into (25), we can derive the following inequality:

$$\begin{aligned}
\mathcal{L}(p_{n+1}) &\leq \mathcal{L}(p_n) - \eta \langle \mathbf{v}_n, \mathbf{Cv}_n \rangle_{L^2(p_n)} + \int_0^\eta (\eta - t) \kappa \langle \mathbf{v}_n, \mathbf{Cv}_n \rangle_{L^2(p_n)} dt \\
&= \mathcal{L}(p_n) - \eta \langle \mathbf{v}_n, \mathbf{Cv}_n \rangle_{L^2(p_n)} + \kappa \frac{\eta^2}{2} \langle \mathbf{v}_n, \mathbf{Cv}_n \rangle_{L^2(p_n)} dt
\end{aligned}$$

This completes the proof. \square

A.3 Derivation of GFlow-VI and NGFlow-VI for Gaussian mean-field Variance Inference

In this section we derive updates for GFlow-VI and NGFlow-VI. For the fist case $\mathbf{C} = \mathbf{I}$, let recall $\boldsymbol{\lambda}_{k,n} = (\boldsymbol{\lambda}_{k,n}, \mathbf{s}_{k,n})$ and mean $\boldsymbol{\lambda}_{k,n}$ and vector $\mathbf{s}_{k,n}$ are updated as follows (see (16)):

$$\begin{aligned}
\boldsymbol{\mu}_{k,n+1} &= \boldsymbol{\mu}_{k,n} - \eta \nabla_{\boldsymbol{\mu}_k} \mathbb{E}_{\mathbf{z} \sim q(\cdot | \boldsymbol{\lambda}_{k,n})} [f(\mathbf{z}) + \log q_n(\mathbf{z})] \\
\mathbf{s}_{k,n+1} &= \mathbf{s}_{k,n} - \eta \nabla_{\mathbf{s}_k} \mathbb{E}_{\mathbf{z} \sim q(\cdot | \boldsymbol{\lambda}_{k,n})} [f(\mathbf{z}) + \log q_n(\mathbf{z})]
\end{aligned}$$

We denote $G = \mathbb{E}_{\mathbf{z} \sim q(\cdot | \boldsymbol{\lambda}_{k,n})} [f(\mathbf{z}) + \log q_n(\mathbf{z})]$. We can estimate the gradients of G with respect to $\boldsymbol{\mu}_k$ and \mathbf{s}_k as follows:

$$\begin{aligned}
\nabla_{\boldsymbol{\mu}_k} G &= \int_{\mathbf{z}} \nabla_{\boldsymbol{\mu}_k} q(\mathbf{z} | \boldsymbol{\lambda}_{k,n}) [f(\mathbf{z}) + \log q_n(\mathbf{z})] d\mathbf{z} + \int_{\mathbf{z}} q(\mathbf{z} | \boldsymbol{\lambda}_{k,n}) \nabla_{\boldsymbol{\mu}_k} \log q_n(\mathbf{z}) d\mathbf{z} \\
&= - \int_{\mathbf{z}} \nabla_{\mathbf{z}} q(\mathbf{z} | \boldsymbol{\lambda}_{k,n}) [f(\mathbf{z}) + \log q_n(\mathbf{z})] d\mathbf{z} + \int_{\mathbf{z}} q(\mathbf{z} | \boldsymbol{\lambda}_{k,n}) \frac{q(\mathbf{z} | \boldsymbol{\lambda}_{k,n}) \nabla_{\boldsymbol{\mu}_k} \log q(\mathbf{z} | \boldsymbol{\lambda}_{k,n})}{q_n(\mathbf{z})} d\mathbf{z} \\
&= \int_{\mathbf{z}} q(\mathbf{z} | \boldsymbol{\lambda}_{k,n}) [\nabla_{\mathbf{z}} f(\mathbf{z}) + \nabla_{\mathbf{z}} \log q_n(\mathbf{z})] d\mathbf{z} + \int_{\mathbf{z}} q(\mathbf{z} | \boldsymbol{\lambda}_{k,n}) \mathbf{w}_k(\mathbf{z}) \nabla_{\boldsymbol{\mu}_k} \log q(\mathbf{z} | \boldsymbol{\lambda}_{k,n}) \\
&= \mathbb{E}_{\mathbf{z} \sim q(\cdot | \boldsymbol{\lambda}_{k,n})} [\nabla_{\mathbf{z}} f(\mathbf{z}) + \nabla_{\mathbf{z}} \log q_n(\mathbf{z}) + \mathbf{w}_k(\mathbf{z}) \nabla_{\boldsymbol{\mu}_k} \log q(\mathbf{z} | \boldsymbol{\lambda}_{k,n})],
\end{aligned} \tag{30}$$

where $\mathbf{w}_k(\mathbf{z}) = q(\mathbf{z} | \boldsymbol{\lambda}_{k,n}) / q_n(\mathbf{z})$. In the second equality, we have used the identity $\nabla_{\boldsymbol{\mu}} q(\mathbf{z} | \boldsymbol{\lambda}) = -\nabla_{\mathbf{z}} q(\mathbf{z} | \boldsymbol{\lambda})$ for q being a Gaussian distribution; in the third equality, we have used the integration by parts for the first term and $\nabla_{\boldsymbol{\mu}} q(\mathbf{z} | \boldsymbol{\lambda}) = q(\mathbf{z} | \boldsymbol{\lambda}) \nabla_{\boldsymbol{\mu}} \log q(\mathbf{z} | \boldsymbol{\lambda})$ for the second term.

$$\begin{aligned}
\nabla_{\mathbf{s}_k} G &= -1 \oslash (\mathbf{s}_{k,n} \odot \mathbf{s}_{k,n}) \odot \int_{\mathbf{z}} \nabla_{\boldsymbol{\sigma}_k^2} q(\mathbf{z} | \boldsymbol{\lambda}_{k,n}) [f(\mathbf{z}) + \log q_n(\mathbf{z})] d\mathbf{z} + \int_{\mathbf{z}} q(\mathbf{z} | \boldsymbol{\lambda}_{k,n}) \nabla_{\mathbf{s}_k} \log q_n(\mathbf{z}) d\mathbf{z} \\
&= -1 \oslash (\mathbf{s}_{k,n} \odot \mathbf{s}_{k,n}) \odot \int_{\mathbf{z}} q(\mathbf{z} | \boldsymbol{\lambda}_{k,n}) \frac{1}{2} \text{diag} [\nabla_{\mathbf{z}}^2 f(\mathbf{z}) + \nabla_{\mathbf{z}}^2 \log q_n(\mathbf{z})] d\mathbf{z} + \int_{\mathbf{z}} q(\mathbf{z} | \boldsymbol{\lambda}_{k,n}) \frac{q(\mathbf{z} | \boldsymbol{\lambda}_{k,n}) \nabla_{\mathbf{s}_k} \log q(\mathbf{z} | \boldsymbol{\lambda}_{k,n})}{q_n(\mathbf{z})} d\mathbf{z} \\
&= \mathbb{E}_{\mathbf{z} \sim q(\cdot | \boldsymbol{\lambda}_{k,n})} \left[-\frac{1}{2} \oslash (\mathbf{s}_{k,n} \odot \mathbf{s}_{k,n}) \odot \text{diag} [\nabla_{\mathbf{z}}^2 f(\mathbf{z}) + \nabla_{\mathbf{z}}^2 \log q_n(\mathbf{z})] + \mathbf{w}_k(\mathbf{z}) \nabla_{\mathbf{s}_k} \log q(\mathbf{z} | \boldsymbol{\lambda}_{k,n}), \right]
\end{aligned} \tag{31}$$

where we have used the change of variable formula in the first equation, the relation (18) for the first term of the second equation. By drawing a sample \mathbf{z} from $q(\mathbf{z}|\boldsymbol{\lambda}_{k,n})$, we have the update of GFlow-VI ((17) in the main text).

Next we derive the update of NGFlow-VI ($\mathbf{C} = \mathbf{F}^{-1}$). We consider $\boldsymbol{\lambda}_k$ to be the natural parameter of the mean-field Gaussian $q(\mathbf{z}|\boldsymbol{\lambda}_k)$. Specifically, the natural parameters and expectation parameters of the k -th Gaussian at the n -th iteration can be defined as follows:

$$\begin{aligned}\boldsymbol{\lambda}_{k,n}^{(1)} &= \mathbf{s}_{k,n} \odot \boldsymbol{\mu}_{k,n}, \boldsymbol{\lambda}_{k,n}^{(2)} = -\frac{1}{2}\mathbf{s}_{k,n} \\ \mathbf{m}_{k,n}^{(1)} &= \boldsymbol{\mu}_{k,n}, \mathbf{m}_{k,n}^{(2)} = \boldsymbol{\mu}_{k,n} \odot \boldsymbol{\mu}_{k,n} + 1 \oslash \mathbf{s}_{k,n}.\end{aligned}$$

Then, the natural parameters are updated as follows (by (19) in the main text):

$$\boldsymbol{\lambda}_{k,n+1} = \boldsymbol{\lambda}_{k,n} - \eta \nabla_{\boldsymbol{\lambda}_k} G$$

Using the chain rule (see Appendix B.1 in [9]), we can express the gradients of G with respect to expectation parameter \mathbf{m}_k in terms of the gradients with respect to $\boldsymbol{\mu}_k$ and $\boldsymbol{\sigma}_k^2$ as follows:

$$\nabla_{\mathbf{m}_k^{(1)}} G = \nabla_{\boldsymbol{\mu}_k} G - 2 \left[\nabla_{\boldsymbol{\sigma}_k^2} G \right] \boldsymbol{\mu}_k, \nabla_{\mathbf{m}_k^{(2)}} G = \nabla_{\boldsymbol{\sigma}_k^2} G$$

By following the derivation in [9], the natural-gradient update is simplified as follows:

$$\mathbf{s}_{k,n+1} = \mathbf{s}_{k,n} + 2\eta \left[\nabla_{\boldsymbol{\sigma}_k^2} G \right]. \quad (32)$$

$$\boldsymbol{\mu}_{k,n+1} = \boldsymbol{\mu}_{k,n} - \eta [\nabla_{\boldsymbol{\mu}_k} G] \oslash \mathbf{s}_{k,n+1}. \quad (33)$$

Using (31), we can derive the full update for $\mathbf{s}_{k,n}$ in (32) as follows:

$$\begin{aligned}\mathbf{s}_{k,n+1} &= \mathbf{s}_{k,n} - 2\eta(\mathbf{s}_{k,n} \odot \mathbf{s}_{k,n}) [\nabla_{\mathbf{s}_k} G] \\ &= \mathbf{s}_{k,n} + \mathbb{E}_{\mathbf{z} \sim q(\cdot|\boldsymbol{\lambda}_{k,n})} [\eta \text{diag} [\nabla_{\mathbf{z}}^2 f(\mathbf{z}) + \nabla_{\mathbf{z}}^2 \log q_n(\mathbf{z})] - 2\eta \mathbf{w}_k(\mathbf{z})(\mathbf{s}_{k,n} \odot \mathbf{s}_{k,n}) \odot \nabla_{\mathbf{s}_k} \log q(\mathbf{z}|\boldsymbol{\lambda}_{k,n})]\end{aligned}$$

Lastly, using (30), we can derive the full update for $\boldsymbol{\mu}_{k,n}$ in (33) as follows:

$$\begin{aligned}\boldsymbol{\mu}_{k,n+1} &= \boldsymbol{\mu}_{k,n} - \eta [\nabla_{\boldsymbol{\mu}_k} G] \oslash \mathbf{s}_{k,n+1} \\ &= \boldsymbol{\mu}_{k,n} - \eta \mathbb{E}_{\mathbf{z} \sim q(\cdot|\boldsymbol{\lambda}_{k,n})} [\nabla_{\mathbf{z}} f(\mathbf{z}) + \nabla_{\mathbf{z}} \log q_n(\mathbf{z}) + \mathbf{w}_n(\mathbf{z}) \nabla_{\boldsymbol{\mu}_k} \log q(\mathbf{z}|\boldsymbol{\lambda}_{k,n})] \oslash \mathbf{s}_{k,n+1}.\end{aligned}$$

By drawing a sample \mathbf{z} from $q(\mathbf{z}|\boldsymbol{\lambda}_{k,n})$, we have the update of NGFlow-VI ((20) in the main text).